

Polymer Crystallization-Driven, Periodic Patterning on Carbon Nanotubes

Lingyu Li,[†] Christopher Y. Li,^{*,†} and Chaoying Ni[‡]

Contribution from the A. J. Drexel Nanotechnology Institute and Department of Materials Science and Engineering, Drexel University, Philadelphia, Pennsylvania 19104, and W. M. Keck Electron Microscopy Facility, Department of Materials Science and Engineering, University of Delaware, Newark, Delaware 19716

Received October 10, 2005; E-mail: chrisli@drexel.edu.

Abstract: We report herein a unique means to periodically pattern polymeric materials on individual carbon nanotubes (CNTs) using a controlled polymer crystallization method. One-dimensional (1D) CNTs were periodically decorated with polymer lamellar crystals, resulting in nano-hybrid shish-kebab (NHSK) structures. The periodicity of the polymer lamellae varies from 20 to 150 nm. The kebabs are approximately 5–10 nm thick (along CNT direction) with a lateral size of ~20 nm to micrometers, which can be readily controlled by varying crystallization conditions. Both polyethylene and Nylon 66 were successfully decorated on single-walled carbon nanotubes (SWNTs), multiwalled carbon nanotubes (MWNTs), as well as vapor grown carbon nanofibers (CNFs). The formation mechanism was attributed to “size-dependent soft epitaxy”. Because NHSK formation conditions depend on CNT structures, it further provides a unique opportunity for CNT separation. The reported method opens a gateway to periodically patterning polymers and different functional groups on individual CNTs in an ordered and controlled manner, an attractive research field that is yet to be explored.

Introduction

Since their discovery,¹ carbon nanotubes (CNTs) have attracted tremendous attention due to their extraordinary mechanical, electrical, and optical properties.^{2–4} Because of the substantial van der Waals attraction, CNTs often form bundles. To manipulate and process CNTs, it is desirable to functionalize the sidewall of CNTs, thereby generating CNT-derivatives that are compatible with solvent as well as organic matrix materials. To this end, both chemical functionalization techniques and noncovalent wrapping methods have been reported.⁵ In chemical functionalization, functional groups are covalently linked to the CNT surface, and it is also referred to as the covalent functionalization method.⁶ The advantage of chemical functionalization is that functional groups are covalently linked to the CNT surface; the linkage is permanent and mechanically stable. However, reaction with the graphitic sheet also results in breaking of the sp² conformation of the carbon atom. The conjugation of the CNT wall is therefore disrupted, and it has been observed that, as compared to the pristine tubes, electrical

and mechanical properties of the chemically functionalized CNT decreased dramatically.^{7,8}

The noncovalent method to functionalize CNTs involves using surfactants, oligomers, biomolecules, and polymers to “wrap” CNTs to enhance their solubility.⁵ Water-soluble polymers such as poly(vinylpyrrolidone) (PVP) and polystyrene sulfonate (PSS) were used to enhance the solubility of CNT in water.⁹ It was proposed that these polymers intimately wrap CNTs, forming a polymer/CNT hybrid material. CNT surface property was altered, and the resulting hybrid materials are soluble in water. The advantage of the noncovalent functionalization is that the integrity of CNT structure is not disrupted and the properties of the CNTs are therefore retained. However, the noncovalent interaction between the wrapping molecules and the CNTs is not as strong as the covalent bonding formed in the chemical functionalization methods.⁵

Our interest is to explore the feasibility of using crystalline polymers to functionalize CNTs via CNT-induced polymer crystallization. If successful, noncovalent functionalization can be achieved and specific chain registry of the polymer upon CNT might occur due to the epitaxial growth of polymer crystals on CNTs. As compared to the reported noncovalent methods, crystalline polymers also possess better mechanical properties, resulting in stronger adhesion between CNT and polymers. The

[†] Drexel University.

[‡] University of Delaware.

- (1) Iijima, S. *Nature* **1991**, *354*, 56–58.
- (2) Thess, A.; Lee, R.; Nikolaev, P.; Dai, H. J.; Petit, P.; Robert, J.; Xu, C. H.; Lee, Y. H.; Kim, S. G.; Rinzler, A. G.; Colbert, D. T.; Scuseria, G. E.; Tomanek, D.; Fischer, J. E.; Smalley, R. E. *Science* **1996**, *273*, 483–487.
- (3) Tans, S. J.; Devoret, M. H.; Dai, H. J.; Thess, A.; Smalley, R. E.; Geerligs, L. J.; Dekker, C. *Nature* **1997**, *386*, 474–477.
- (4) Walters, D. A.; Ericson, L. M.; Casavant, M. J.; Liu, J.; Colbert, D. T.; Smith, K. A.; Smalley, R. E. *Appl. Phys. Lett.* **1999**, *74*, 3803–3805.
- (5) Hirsch, A. *Angew. Chem., Int. Ed.* **2002**, *41*, 1853–1859.
- (6) Banerjee, S.; Hemraj-Benny, T.; Wong, S. S. *Adv. Mater.* **2005**, *17*, 17–29.

- (7) Garg, A.; Sinnott, S. B. *Chem. Phys. Lett.* **1998**, *295*, 273–278.
- (8) Bekyarova, E.; Itkis, M. E.; Cabrera, N.; Zhao, B.; Yu, A. P.; Gao, J. B.; Haddon, R. C. *J. Am. Chem. Soc.* **2005**, *127*, 5990–5995.
- (9) O’Connell, M. J.; Boul, P.; Ericson, L. M.; Huffman, C.; Wang, Y. H.; Haroz, E.; Kuper, C.; Tour, J.; Ausman, K. D.; Smalley, R. E. *Chem. Phys. Lett.* **2001**, *342*, 265–271.

degree of functionalization could also be easily controlled by tuning the crystal size (see following sections).

Previous research shows that carbon materials, in various forms, are able to induce polymer crystallization. The following three types of related research can be summarized regarding polymer crystallization induced by carbon materials.

Epitaxial Growth of Polymer on Highly Ordered Pyrolytic Graphite (HOPG). Sano et al. observed the epitaxial growth of polymers such as Nylon 6, poly(tetrahydrofuran), poly(oxacyclobutane), and poly(ethylene oxide), etc. on graphite surface using scanning tunneling microscopy (STM) and atomic force microscopy (AFM) techniques.¹⁰ These polymer chains have been found to possess a trans conformation and align parallel to the (10-10) or (11-20) direction of the graphite lattice. Graphite-induced polyethylene (PE) crystallization was also reported.¹¹

Carbon Fiber (CF)-Induced Polymer Crystallization. To achieve the CF-reinforced polymer composite, CFs, which are $\sim 10 \mu\text{m}$ in diameter, have been used extensively to induce polymer crystallization (so-called transcrystallization). It has also been demonstrated that a number of polymers [such as isotactic polypropylene (iPP), PE, Nylon 66, poly(phenylene sulfide), etc.] can epitaxially grow on the CF surface.^{12,13}

CNT-Induced Polymer Crystallization. Recently, polymer CNT nanocomposites (PCNs) formed by CNTs and semicrystalline polymers such as iPP,¹⁴ PE,¹⁵ poly(vinyl alcohol) (PVA),¹⁶ polyacrylonitrile (PAN),¹⁷ and thermoplastic elastomers such as polyurethane have been studied.¹⁸ Using DSC nonisothermal and isothermal crystallization techniques, it has been found that $t_{1/2}$ decreases with increasing CNT content in PCNs, indicating that CNT could induce polymer crystallization.

All of these previous works warrant the feasibility of using crystalline polymer to functionalize CNTs. To clearly view the CNT/polymer interface, we proposed the use of a controlled solution crystallization method. Polymer single-crystal functionalized CNTs were recently observed.¹⁹ In our recent communication,¹⁹ we reported the first observation of the polymer single-crystal-decorated CNTs. Solution crystallization was used. PE and Nylon 66 were found to be able to periodically grow on CNT surfaces. In this Article, we report the systematic study on polymer crystallization-driven CNT functionalization (PCCF). Three main points will be discussed: (1) The novel PCCF technique is a generic method for CNT functionalization. It can be used for a variety of CNTs, including single-walled (SWNT), multiwalled (MWNT), and vapor grown carbon nanofibers (CNF). Both PE and Nylon 66 were used as the model crystalline polymers, leading to either a hydrophobic or a hydrophilic CNT surface. (2) The formation mechanism of this unique structure was attributed to “size-dependent soft

epitaxy” (SSE). Two main factors affected the polymer chain orientation on CNT during crystal growth: epitaxy and geometry confinement. As the diameter of the CNT is comparable to the radius of gyration of a polymer chain, its highly curved surface leads to strong geometric confinement and polymer chains are forced to align parallel to the CNT axis upon crystallization, regardless of the CNT chirality. Because strict crystal lattice matching between the CNT surface and the polymer crystals was not required, “soft epitaxy” was adopted to describe this unique growth mechanism. As the diameter increases to $\sim 100\text{--}300 \text{ nm}$, the geometric confinement effect became weakened and epitaxy dictated the polymer lamellar growth. (3) As the formation condition of this novel hybrid structure is highly sensitive to CNT structures, PCCF might be used for CNT separation. MWNTs with different diameters/structures were used to demonstrate this concept.

Results and Discussion

Polymer Crystallization-Driven Periodic Functionalization of CNTs, a Generic Method. PE-Decorated SWNTs. To modify the CNT surface and realize controlled functionalization, a polymer solution crystallization technique was employed. PE was used as the model polymer. *p*-Xylene was used as the solvent for controlled solution crystallization.²⁰ Figure 1 shows two TEM images of PE-decorated SWNTs after solution crystallization at $104 \text{ }^\circ\text{C}$ for 30 min. Note that the solution was not under an extension or shear flow field. The relatively high T_c , which is higher than the clearing temperature of PE in *p*-xylene, was chosen so that homogeneous nucleation of PE was prohibited, and all of the PE crystals grown at this condition were initiated by CNTs via a heterogeneous nucleation mechanism. It is evident from the figure that CNTs are decorated with disc-shaped objects (arrows), which are PE single-crystal lamellae (edge-on views). The crystalline nature of the disc-shaped objects can also be confirmed by differential scanning calorimetry and wide-angle X-ray experiments as shown in the Supporting Information (Figure S.1). The average lateral dimension is $\sim 50\text{--}80 \text{ nm}$. It is of great interest that these PE lamellae were strung together by SWNTs with the average periodicity of $\sim 40\text{--}50 \text{ nm}$. This fibril-linked-disk structure is similar to the classic “shish-kebab” polymer crystals formed under shear field, as was first observed in the 1960s by Geil and Reneker (“Hedgerow”)²⁰ and Pennings.²¹ A shish-kebab polymer crystal usually consists of a central fibril (shish) and disc-shaped folded-chain lamellae (kebab) oriented perpendicularly to the shish as shown in Figure 2a. Figure 2b shows the schematic representation of the structure in Figure 1. A few similarities between these two structures can be found from this figure: (1) Both structures possess a central fibril core and the diameter of the core is approximately one to a few tens nanometers. (2) The central cores in both structures are wrapped with disc-shaped single crystals with the lamellar thickness of several to a few tens nanometers. (3) Single-crystal lamellae are perpendicular to the shish axis. (4) These lamellae are periodically located on the central one-dimensional (1D) cores. Because the central shish is CNT while the kebabs are formed by PE single crystals in Figure 2b, we name this novel structure nano-hybrid shish-kebab (NHSK).

(10) Sano, M.; Sasaki, D. Y.; Kunitake, T. *Science* **1992**, *258*, 441–443.

(11) Tuinstra, F.; Baer, E. *J. Polym. Sci., Polym. Lett.* **1970**, *8*, 861–865.

(12) Khoury, F. *Proc. SPE* **1990**, 1261–1263.

(13) Hsiao, B. S.; Chen, E. J. H. *MRS Symp. Proc.* **1990**, *170*, 117–121.

(14) Grady, B. P.; Pompeo, F.; Shambaugh, R.; Resasco, D. E. *J. Phys. Chem. B* **2002**, *106*, 5852–5858.

(15) Haggenueller, R.; Gommans, H. H.; Rinzler, A. G.; Fischer, J. E.; Winey, K. I. *Chem. Phys. Lett.* **2000**, *330*, 219–225.

(16) Shaffer, M. S. P.; Windle, A. H. *Adv. Mater.* **1999**, *11*, 937–941.

(17) Ko, F.; Gogotsi, Y.; Ali, A.; Naguib, N.; Ye, H. H.; Yang, G. L.; Li, C.; Willis, P. *Adv. Mater.* **2003**, *15*, 1161–1165.

(18) Koerner, H.; Price, G.; Pearce, N. A.; Alexander, M.; Vaia, R. A. *Nat. Mater.* **2004**, *3*, 115–120.

(19) Li, C. Y.; Li, L. Y.; Cai, W. W.; Kodjie, S. L.; Tenneti, K. K. *Adv. Mater.* **2005**, *17*, 1198–1202.

(20) Geil, P. H. *Polymer single crystals*; Robert E. Krieger Pub.: Juntington, NY, 1973.

(21) Pennings, A. J.; Kiel, A. M. *Kolloid Z. Z. Polym.* **1965**, *205*, 160–162.

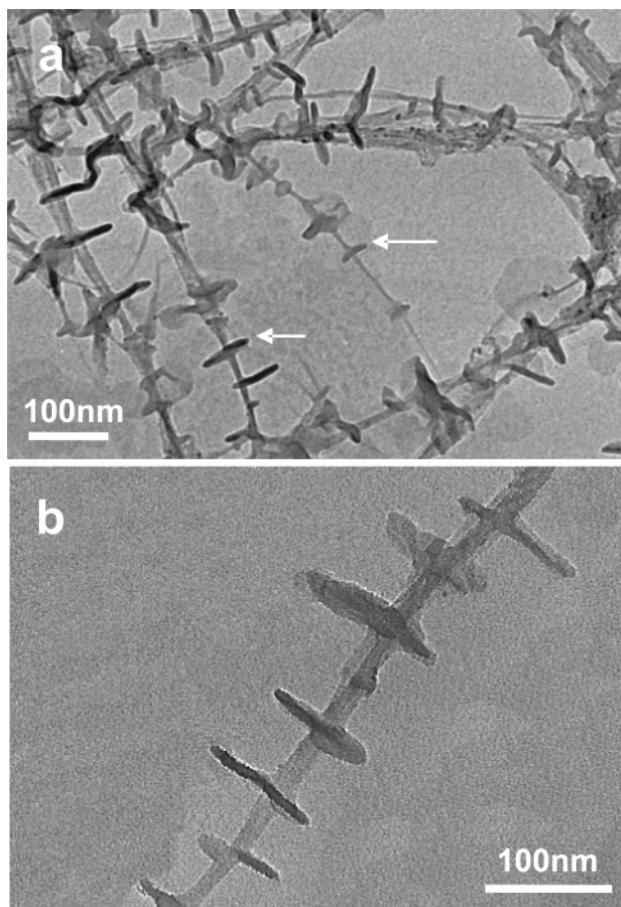


Figure 1. TEM micrograph of SWNTs periodically patterned with PE lamellae crystals produced by crystallization of PE on SWNTs at 104 °C in *p*-xylene for 0.5 h (a). The PE and SWNT concentrations are 0.01 wt % and 0.002 wt %, respectively. SWNT bundles can be seen in NHSK as shown in (b).

Conventional polymer shish-kebab structure is formed in polymer solution/melt under an external shear field. For a polymer solution (i.e., 5% polyethylene/xylene) under an extension/shear flow, polymer chains that normally possess a coil conformation might undergo a coil-to-stretch transition.²² If the chain is longer than a critical molecular weight (M^*), the stretched polymer chains aggregate to form extended chain fibrillar crystals.²³ The remaining coil polymer chains could then crystallize upon the fibrillar crystals in a folded periodic fashion, forming the shish-kebab morphology. The stretched polymers are the shish, and the folded lamellae are kebabs. In this study, the SWNT/PE solution was not under extension or shear flow during crystallization. Because the nano fibrillar structure of SWNT provides a 1D nucleation surface, shear is not needed in the CNT-induced crystallization and formation of NHSK was observed. It is noticeable that some of the SWNTs are in the form of small bundles. Figure 1b shows an enlarged NHSK image, and it is evident that the central shish consists of a bundle of SWNTs. This is because as the polymer chains started to nucleate on SWNTs, due to the poor solubility of SWNT in *p*-xylene, SWNTs were not completely exfoliated. A fraction of the SWNTs were still in the bundle state, and PE crystallized/wrapped the bundle, which in turn captured the “state of the

CNT agglomeration” in *p*-xylene solution. This image, therefore, can be considered as the direct visualization of the degree of CNT exfoliation in *p*-xylene. PE NHSK with better exfoliated SWNTs can be achieved by using 1,2-dichlorobenzene (DCB) as the solvent, which will be discussed in the following section.

The observation of NHSK opens the gateway to periodically functionalizing CNTs. Periodic functionalization of CNTs is an attractive field of research, and it provides a unique opportunity to pattern 1D CNTs to create functional, ordered structures for electrical and optical applications. Periodic functionalization of CNTs, on the other hand, is an extremely challenging task due to the small size of CNTs. Very few reported CNT functionalization research works have been dedicated to studying how the functional groups arrange on the CNT surface. Recently, Worsley et al. carefully investigated the structure of the CNTs functionalized by the Bingel reaction.²⁴ The authors were able to identify long-range, regular patterns of the functional groups on the individual CNT surfaces. When functionalized, the formation of the sp^3 cyclopropane structure results in the disruption in the sp^2 lattice, altering the electronic properties of the nanotube and leading to a larger band gap depending on the degree of functionalization. Well-resolved images of individual functional groups on a nanotube bundle were reported with a clear periodicity of ~ 4.6 nm. In the present NHSK case, it is evident that PCCF also led to periodic functionalization of CNTs. Furthermore, as compared to the previous reported techniques, PCCF is unique because (1) it provides periodic functionalization and the periodicity is tunable from 20 to 150 nm (see following sections), as opposed to 4.6 nm in the Bingel reaction-induced periodic functionalization; (2) it belongs to the noncovalent functionalization type and CNT integrity remained; (3) a variety of functional groups could be introduced on the chain ends and then brought to the vicinity of the CNT (Figure 2b); and (4) the degree of functionalization could be easily controlled simply by increasing the kebab size. In the following section, we shall focus on the generality of the newly discovered method, which is demonstrated by the applicability of PCCF in a variety of CNTs as well as polymers.

From SWNT to MWNT/CNF. To demonstrate the generality of this PCCF method, different kinds of CNTs were employed in this study as shown in Table 1.

First, MWNTs synthesized by arc discharge and CVD methods were used. The diameters of these MWNTs were reported as 5–15 and 20–30 nm, respectively. They are thus denoted as MWNT-10 and MWNT-25. Figure 3a shows the TEM image of the resulting PE functionalized MWNT-10s after solution crystallization in *p*-xylene at 103 °C for 30 min, and the PE concentration was 0.01 wt %. It is evident that the disc-shaped PE single-crystal lamellae were periodically located along the tube axis and they are mostly perpendicular to the tube axis. A larger periodicity (the average periodicity is about 50–70 nm) is observed as compared to that in SWNTs, and the diameter of kebab is about 50–70 nm. NHSK with better dispersed MWNT-10 can also be achieved by using DCB as the solvent, which will be discussed in the following section.

Figure 3b shows PE functionalized MWNT-25s (*p*-xylene was the solvent and $T_c = 97$ °C). The tubes are slightly curvy and possess more defects as opposed to MWNTs synthesized

(22) De Gennes, P. G. *J. Chem. Phys.* **1970**, *60*, 5030–5042.

(23) Somani, R. H.; Hsiao, B. S.; Nogales, A.; Fruitwala, H.; Srinivas, S.; Tsou, A. H. *Macromolecules* **2001**, *34*, 5902–5909.

(24) Worsley, K. A.; Moonosawmy, K. R.; Kruse, P. *Nano Lett.* **2004**, *4*, 1541–1546.

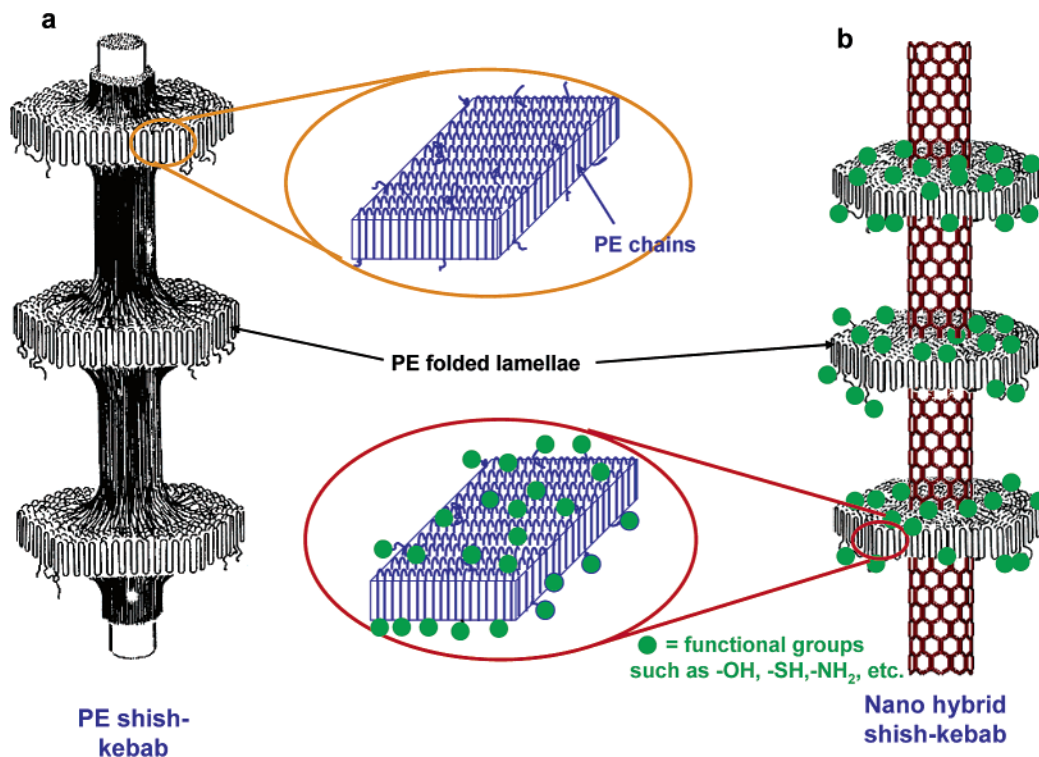


Figure 2. Schematic representations of (a) polymer shish-kebab crystals; (b) PE/CNT nano-hybrid shish-kebab structure. Periodic patterning of different functionalities can be achieved by crystallizing polymers with different end groups such as -OH, -SH, -NH₂. These end groups are “defects” for the polymer single crystals and will most likely be excluded onto the crystal surfaces as shown in (b). The degree of functionalization can be easily controlled by tuning polymer crystal sizes.

Table 1. Source of CNTs

category	synthetic method	vendor	outer diameter	length
SWNT	HiPCO	Carbon Nanotechnology, Inc.	0.8–1.3 nm	~micrometer
MWNT-10 (product #406074)	arc discharge	Sigma	5–15 nm	1–10 μm
MWNT-25 (product #1240XH)	CVD	Nanostructured & Amorphous Materials, Inc.	20–30 nm	0.5–2 μm
CNF (PR-19-HHT)	CVD	Applied Science, Inc.	100–300 nm	30–100 μm

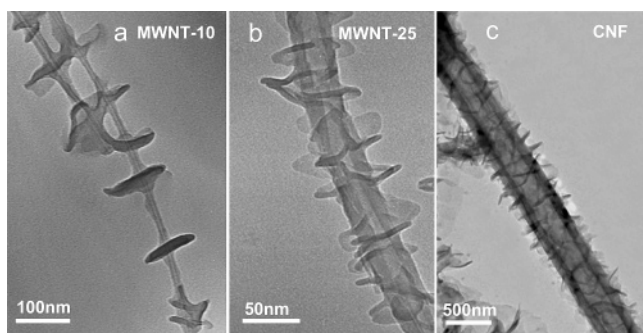


Figure 3. TEM images of PE/MWNT-10 NHSK (a), PE/MWNT-25 NHSK (b), and PE/CNF NHSK structures produced by crystallization of PE on different CNTs and CNF in *p*-xylene for 0.5 h at 103, 97, and 97 °C. The PE, MWNT, and CNF concentrations are 0.01, 0.002, and 0.002 wt %, respectively.

by the arc discharge method and HiPCO SWNTs. However, NHSK structure is clearly seen from the figure. The outer diameter of MWNT-25 is about 30 nm. The disc-shaped PE single-crystal lamellae were located along the tube axis and not as uniform as those on MWNT-10s, which is probably due to the defects on the MWNT-25 surface and/or relatively lower T_c . Less perfect sidewall structure is also believed to be the reason that the kebab periodicity was not as well formed as in MWNT-10.

To further demonstrate the generality of this method, much larger size CNFs were used. CNFs are attractive from the practical point of view due to their relatively low cost. These CNFs have an outer diameter of 100–300 nm, a hollow core, and length on the order of 30–100 μm . Figure 3c shows a TEM image of the PE NHSK with CNF shish. *p*-Xylene was used, and T_c was 97 °C. It is clear that PE forms single-crystal lamellae on the central CNF. The PE lamellae in this case are large; the diameter is about 500 nm.

From these three figures, it is evident that PE was successfully used to form NHSK structure with CNTs having diameters ranging from less than 1 to ~300 nm. A unique feature of the NHSKs is that the degree of functionalization can be easily tuned by changing the experimental parameters. Much larger kebabs can be obtained by crystallizing PE/MWNT-10 mixture in *p*-xylene with relatively higher PE concentration at 103 °C for 30 min as shown in the Supporting Information (Figure S.2). Larger kebab surface ensures more functional groups as indicated in Figure 2b. Furthermore, as compared to pristine CNTs, by choosing polymers that are miscible with the kebabs, these NHSKs are easier to disperse in a polymer matrix, leading to controllable CNT nanocomposites. Research work on the nanocomposites fabricated using NHSKs is ongoing.

Nylon 66-Decorated CNTs. Because the polymer used in PCCF dictates the surface properties of the final NHSK, it is of

interest to modify CNT surface using different polymers in addition to PE. Nylon 66 was used as the second model material for three reasons: (1) PE is relatively hydrophobic, and using Nylon 66 could lead to NHSKs with relatively hydrophilic surface. (2) Nylon 66 possesses a zigzag conformation, and it is anticipated that this planar chain conformation might facilitate NHSK formation. (3) It has been reported that Nylon 6 could epitaxially grow on HOPG surface.¹⁰ Glycerin was used as the solvent for Nylon 66 single-crystal growth, and T_c was chosen to be 185 °C.²⁵ Figure S.3 in the Supporting Information shows an SEM image of Nylon 66/MWNT-10s NHSKs. Based on Figure S.3 and the TEM results (not shown), all of the MWNTs have been separated into individual tubes and periodically decorated with Nylon 66 lamellar crystals along the entire tube. Note that the kebab-like structures appear to be “thick” in the figure because they are sputtered with Pt. The periodicity of the kebab-like structures is $\sim 20\text{--}30$ nm, which is different from PE/MWNT-10 NHSKs, suggesting that the periodicity also depends on the nature of the decorating polymers. While PE NHSK possesses a hydrophobic surface, the surface of Nylon 66 NHSKs is more hydrophilic. Nylon 66 was also crystallized on SWNTs to test the generality of the method. The upper-right inset of Figure S.3 shows a shadowed TEM image of a Nylon 66/SWNT NHSK crystallized at 188 °C for 1 h. A periodic array of the Nylon 66 single crystals again is evident. The lateral dimension of the kebab-like structure is ~ 20 nm, and the periodicity is $\sim 20\text{--}30$ nm. Therefore, NHSKs with relatively hydrophilic Nylon 66 surface were achieved. This further shows that PCCF is a generic technique for CNT functionalization.

NHSK Formation Mechanism. Size-Dependent Soft Epitaxy (SSE). Forming NHSK on CNTs is intriguing. One key observation with conventional PE shish-kebab-like structures is that the polymer chains in the kebab-like structures are parallel to the shish axis, leading to the orthogonal orientation between lamellar surface and the shish axis. This observation also holds in the present case. It is of interest that orthogonal orientation was observed in PE NHSK because the chirality of CNT could significantly affect NHSK structure. We postulate that there are two possible factors that affect NHSK growth: first, epitaxial growth of PE on CNT. A strict crystallographic relationship is needed between the polymer chain and the graphitic lattice. Second, geometric confinement by the CNT also plays a role. Because of their small diameters, CNTs themselves can be considered as rigid macromolecules and polymer chains might prefer to align along the tube axis regardless of the lattice matching between the polymer chain and the graphitic sheet. This mechanism can be attributed to “soft epitaxy”, in which strict lattice matching is not required. We speculate that the true growth might involve both and is size-dependent, as shown in Figure 4. A typical polymer possesses a radius of gyration of ~ 10 nm (PE ~ 100 K g/mol, $R_g \approx 13.8$ nm assuming the θ condition).²⁶ As a macromolecule of such a size diffuses to the fiber/tube surface and crystallizes, the diameter of the fiber/tube plays a critical role in crystal formation. For larger diameter fibers (i.e., CF, 10 μm in diameter), the surface curvature is small and the polymer behaves as if it is on a flat surface. Strict lattice match and epitaxy should be the main growth mechanism. For smaller

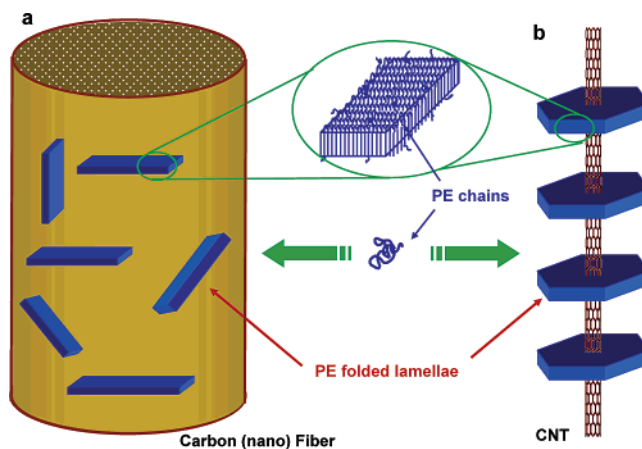


Figure 4. Schematic representation of the proposed “size-dependent soft epitaxy” mechanism. For large-diameter CNFs, PE lamellae are randomly orientated on the fiber surface (a), while for small diameter CNTs, soft epitaxy dictates the parallel orientation between PE chains and the CNT axis, leading to an orthogonal orientation between CNT and PE lamellar surface (b).

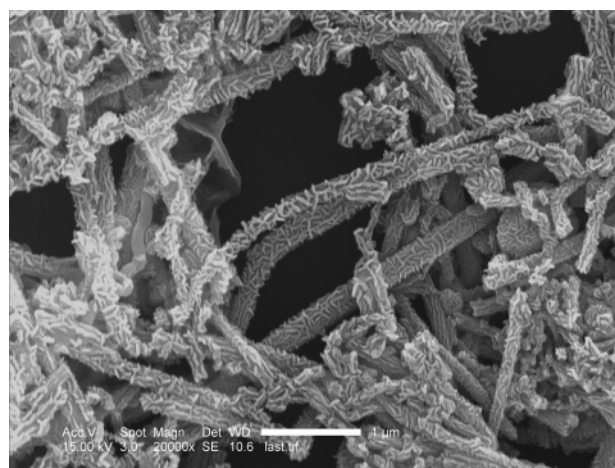


Figure 5. SEM micrograph of PE periodically functionalized CNFs produced by crystallization of PE on CNTs at 97 °C in *p*-xylene for 0.5 h. Random orientation of PE lamellae can be clearly seen on the CNF surface. The PE and CNF concentrations are 0.01 and 0.002 wt %, respectively.

fibers, as the fiber diameter approaches R_g of the polymer chain, the fiber surface is “molecularly curvy”. This curvy surface substantially affects the stability of the crystals if the polymer chain and the fiber axis do not match, which would lead to curved crystals with distorted lattice. Therefore, as a polymer starts to crystallize on this surface, two scenarios could occur (using PE as an example, in which case epitaxy requires the PE chain $\langle 001 \rangle$ to be parallel with $\langle 2\text{-}1\text{-}10 \rangle$ graphite):^{11,27} (1) If the lattice of the graphitic sheet orients in such a way that $\langle 2\text{-}1\text{-}10 \rangle$ is parallel to the CNT axis [an (n, n) tube], both lattice matching and the geometric confinement dictate the polymer chain to be parallel with the CNT axis. (2) If $\langle 2\text{-}1\text{-}10 \rangle$ is not parallel to the CNT axis [an (n, m) tube, $n \neq m$], lattice matching and geometric confinement therefore compete with each other, and the dominant factor should determine the chain orientation. Because the geometric confinement becomes more significant as the fiber diameter decreases, one can envisage that for CNTs with small fiber diameter, geometric confinement would be the major factor and polymer chains should be exclusively parallel

(25) Cai, W. W.; Li, C. Y.; Li, L. Y.; Lotz, B.; Keating, M. N.; Marks, D. *Adv. Mater.* **2004**, *16*, 600–605.

(26) Flory, P. J. *Principles of polymer chemistry*; Cornell University Press: Ithaca, NY, 1953.

(27) Takenaka, Y.; Miyajiri, H.; Hoshino, A.; Tracz, A.; Jeszka, J. K.; Kucinska, I. *Macromolecules* **2004**, *37*, 9667–9669.

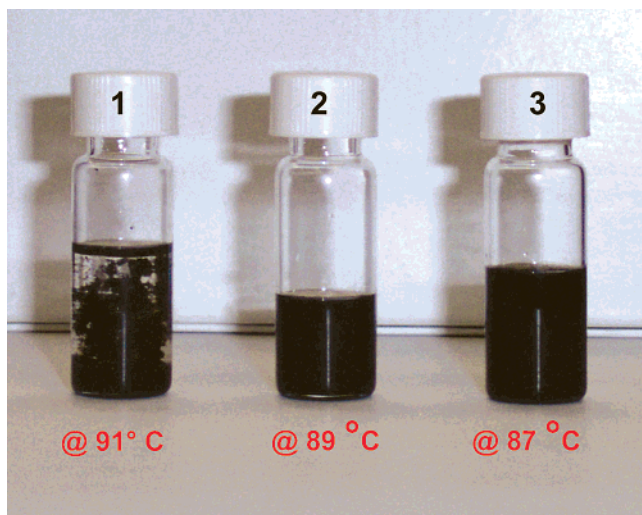


Figure 6. Appearance of three samples made by crystallizing PE in dichlorobenzene (DCB) in the presence of SWNT at different temperatures (91, 89, and 87 °C). The PE and SWNT concentrations are 0.01 and 0.02 wt %, respectively.

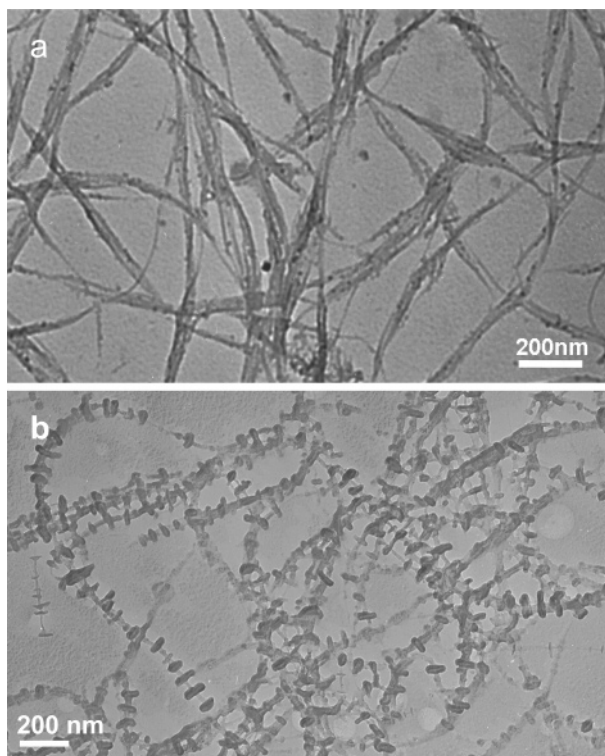


Figure 7. TEM micrograph of PE periodically functionalized SWNTs produced by crystallization of PE on SWNTs in DCB at different temperatures for 1 h. Part (a) shows that at 91 °C, PE did not crystallize in DCB. Part (b) shows that at 89 °C, PE periodically functionalized SWNTs and NHSK were formed. The PE and SWNT concentrations are 0.01 and 0.02 wt %, respectively.

to the CNT axis, disregarding the CNT chirality. As a consequence, kebab crystal lamellae should be perpendicular to the CNT axis, and orthogonal orientation was obtained. For larger diameter CNFs, geometric confinement is weak, and lattice matching might play the major role and dictate the orientation of the polymer chain. Because a variety of graphitic sheet orientations exist for CNFs, epitaxial growth of the polymer crystals would lead to different orientations of the polymer chains/lamellar normal.

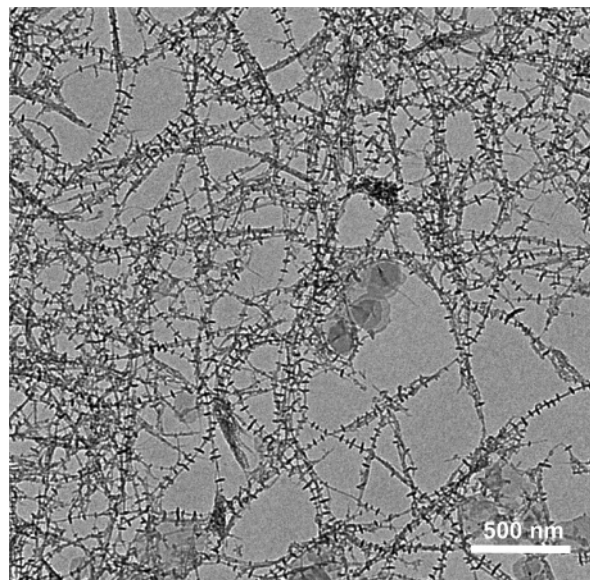


Figure 8. TEM micrograph of PE/SWNT NHSK produced by crystallization of PE on SWNTs in DCB at 88 °C for 3 h. The PE and SWNT concentrations are 0.02 and 0.01 wt %, respectively.

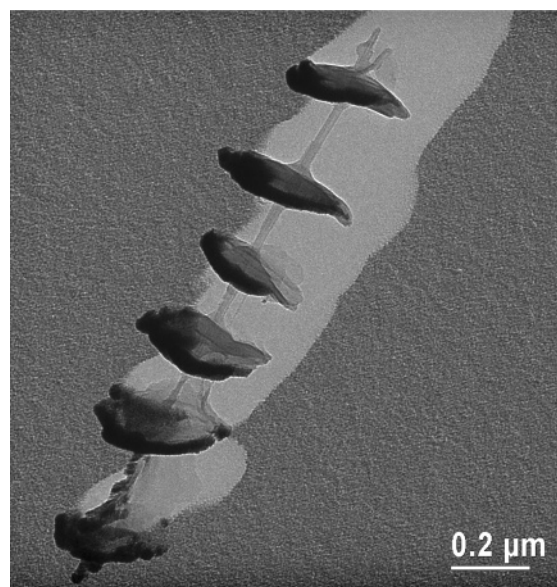


Figure 9. TEM micrograph of PE/SWNT NHSK produced by crystallization of PE on MWNT-10's in DCB at 91 °C for 1 h. The PE and MWNT concentrations are 0.01 and 0.005 wt %, respectively.

To confirm this hypothesis, TEM and SEM experiments were conducted to study the detailed lamellar orientation on the CNT/CNF surface. Figure 3a clearly shows that PE lamellae are perpendicular to the MWNT-10 axis, indicating the polymer chains are parallel to the CNT axis (also see Figures 8, 10a). On the other hand, Figure 5 shows the SEM image of CNF/PE NHSKs. Interestingly, PE lamellae possess multiple orientations: the lamellar normals are parallel, perpendicular, or oblique to the CNF axis. This observation indicates that in CNF samples, because the fiber diameter is relatively large (100–300 nm), the curvature of CNF is not significant for PE macromolecules, and lattice epitaxy is therefore the major factor as CNF-induced crystallization occurs. It should be noted that in Figure 3c, most of the kebabs of the CNF/PE NHSK are nearly perpendicular to the CNF surface; this is probably because adopting this perpendicular orientation could facilitate the PE to grow into

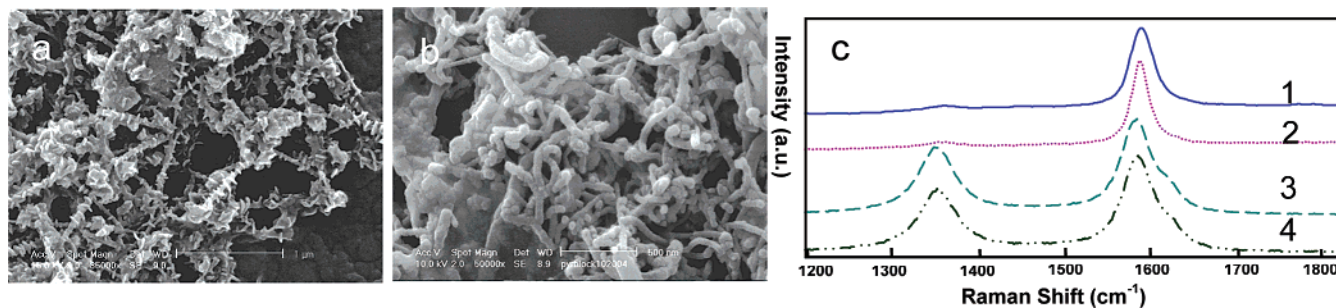


Figure 10. SEM images of (a) supernatant and (b) precipitant resulting from mixed crystallization of PE/MWNT-10/MWNT-25 in *p*-xylene at 103 °C. The PE, MWNT-10, and MWNT-25 concentrations are 0.01, 0.001, and 0.001 wt %, respectively. Part (c) shows Raman spectra of pristine MWNT-10 (2), MWNT-25 (4), the supernatant (1), and the precipitant (3).

larger size crystals. In parallel and oblique orientation, space confinement from the adjacent lamellar crystals might eventually prevent them from growing into large size. Thus, SEM observations clearly support the SSE hypothesis.

NHKS for CNT Dispersion and Separation. Because of the decorating polymer crystals, NHKS can be easily dispersed in solution. To increase the efficiency of functionalization, the initial concentration of SWNTs in the PE solution has to be increased. HiPco SWNT samples were used for this study.²⁸ Bahr et al. demonstrated that DCB is one of the best solvents for SWNTs (~95 mg/L).²⁹ We thus conducted the PE crystallization experiment in DCB. In this case, 1 mg SWNT was dissolved in 1 g of DCB by ultrasonication for about 3 h to prepare the premix (note that the SWNT concentration is much higher than that in *p*-xylene). This premix was added into 4 g of PE/DCB solution at 120 °C, and the final PE concentration is 0.01 wt %. After equilibration for ~10 min, the solution was transferred to a preset T_c . Three different T_c 's (91, 89, and 87 °C) were used, and Figure 6 shows the resulting samples. Note that all three samples have the same SWNT concentration. It is clear that in sample 1, black precipitates were observed within 1 h after crystallization, presumably due to agglomeration of CNTs. On the other hand, samples 2 and 3 appeared to be stable, and did not precipitate 3 months after being prepared. This phenomenon suggested that 91 °C was too high for PE crystallization in DCB; NHKS was not formed in sample 1. In samples 2 and 3, the stable suspension of SWNT indicates that SWNTs were decorated by PE crystals and NHKS structures prevented SWNTs from precipitation. TEM experiment observations were conducted to confirm this hypothesis, and the results are shown in Figure 7. It is evident that Figure 7a (sample 1) contains pristine SWNT bundles without any PE crystals attached while Figure 7b (sample 2) shows NHKS structure and all of the SWNTs were decorated with PE single-crystal lamellae. Similar to the result of PE NHKS formed in *p*-xylene, most of the SWNTs are in bundles. Note that the bundle formation is probably due to the high SWNT concentration we used.

A lower concentration of SWNTs was used to achieve more complete exfoliation between SWNTs. Figure 8 shows that PE NHKSs were obtained from 0.01 wt % SWNT in DCB. It is evident that, as compared to Figure 7, SWNTs are much better separated and all of the SWNTs were decorated with PE crystals.

DCB was also used for a MWNT NHKS study; Figure 9 shows a TEM image of PE/MWNT-10 NHKS prepared in DCB. Note that in Figure 9, the kebab size and periodicity are much larger than that in Figure 3a, indicating that the NHKS structural parameters depend on the crystallization conditions. This provides a unique opportunity to control the periodicity and thus the degree of functionalization of CNTs.

It is also worth noting that the formation temperatures of NHKS depend on the CNT structures. The suitable T_c values for SWNT, MWNT-10, MWNT-25, and CNFs in *p*-xylene are 104, 103, 97, and 97 °C, respectively. Because CNTs that do not form NHKS easily precipitate while NHKS is stable in the solvent, PCCF thus also provides a unique opportunity to achieve CNT separation. To demonstrate this concept, MWNT-10 and MWNT-25 were mixed together in *p*-xylene, and the solution was further mixed with PE and crystallized at 103 °C. It was anticipated that at this T_c , only MWNT-10 NHKS could be formed. It was observed that after 3 h of crystallization, part of the CNT precipitated while the rest was stable in the solution. The supernatant and the precipitant were collected, and SEM was used to study their structure; the results are shown in Figure 10. It is evident that the supernatants are NHKSs and the precipitants are naked CNTs. Of interest is that all of the NHKSs are formed with relatively straight CNTs while the naked CNTs are curly. Because the MWNT-25 is curly while MWNT-10 is straight due to the synthetic procedure, it can therefore be concluded that the supernatant NHKSs are formed by MWNT-10 while the precipitates are MWNT-25, as we anticipated because 103 °C is the right condition for MWNT-10 to form NHKS and MWNT-25 does not induce PE crystallization at this temperature.

To further prove the separation result, Raman spectra were obtained from both the supernatant and precipitant as well as the pristine CNTs as shown in Figure 10c. Spectra 1 and 2 were taken from supernatant and pristine MWNT-10. They have almost the same pattern, indicating that the solution crystallization method does not affect the graphite structure of the MWNTs. A strong peak at 1578 cm^{-1} (G band), which represents the high-frequency E_{2g} Raman scattering mode of sp^2 -hybridized carbon material, and a disordered structure-induced peak at 1352 cm^{-1} (D band), which may originate from the defects in the curved graphene sheets and tube ends, are seen. Raman spectra 3 and 4 are from the sediment collected in the MWNTs separation experiment and pristine MWNT-25. The spectra resembled those reported in the literature for CVD-grown CNT.³⁰ The intensity of the D band is much stronger as

(28) Nikolaev, P.; Bronikowski, M. J.; Bradley, R. K.; Rohmund, F.; Colbert, D. T.; Smith, K. A.; Smalley, R. E. *Chem. Phys. Lett.* **1999**, *313*, 91–97.
 (29) Bahr, J. L.; Mickelson, E. T.; Bronikowski, M. J.; Smalley, R. E.; Tour, J. M. *Chem. Commun.* **2001**, *2*, 193–194.

compared to that of arc-discharged CNT in a and b. The degree of graphitization is an indicator of the carbon nanotubes' disorder level and is characterized by the intensity ratio of the D and G bands ($R \approx I_D/I_G$). The intensity ratios obtained from Raman spectra 1 and 3 in Figure 10c are 0.21 and 0.72, respectively. The values are comparable to those reported for arc-discharged CNT and CVD-grown CNT. Both SEM and Raman experiments thus confirmed that in the CNT separation experiment, supernatant and precipitant consist of MWNT-10 and MWNT-25, respectively, due to the selective crystallization condition that was chosen. Therefore, CNT separation was accomplished by PCCF; detailed work is ongoing to study the selectivity/sensitivity of this unique technique.

Conclusions

In conclusion, we have demonstrated that controlled polymer solution crystallization can be used to synthesize polymer single-crystal-CNT hybrid materials. Lamellar crystals were formed, periodically spaced along entire CNTs. A novel NHSK structure was observed. Because polymers can be easily end-functionalized, this observation led to a unique CNT functionalizing technique, PCCF, which is different from all of the previously reported methods. A variety of CNTs and two different polymers were used for NHSK formation, indicating that PCCF is a generic method for CNT functionalization. The degree of

functionalization can be easily controlled by tuning the crystallization condition, and the resulting NHSK also possesses the unique periodic structure, opening the possibility for periodic nano patterning. The formation mechanism of the NHSK was attributed to SSE. For small diameter CNTs, geometric confinement dictates the polymer chain orientation in the kebabs, and exclusively orthogonal orientation between PE lamellar surface and CNT axis was observed. As the diameter increases, normal epitaxy growth plays a major role, and multiple orientations of PE lamellae were observed. Because the formation conditions of the NHSK depend on the CNT structures, PCCF was also successfully used for CNT separation. MWNT-10 and MWNT-25 were successfully separated. It is envisaged that PCCF could also be used for functionalizing other 1D nanowire systems; this is currently under investigation.

Acknowledgment. This work was supported by the NSF CAREER award (DMR-0239415), DMI-0508407, ACS-PRF, 3M, and DuPont. Supply of Nylon 66 samples from DuPont (Dr. Mimi Keating) is appreciated. The ESEM was purchased through the support of the NSF (BES-0216343).

Supporting Information Available: Experimental section, DSC and XRD data of NHSK, and SEM and TEM images of PE and Nylon 66 NHSK. This material is available free of charge via the Internet at <http://pubs.acs.org>.

(30) Kwok, K.; Chiu, W. K. S. *Carbon* **2005**, *43*, 437–446.

JA056923H